JOURNAL OF GEOPHYSICAL RESEARCH, VOL. 101, NO. D14, PAGES 19,169–19,174, AUGUST 27, 1996

Hodographic analysis of gravity waves: Relationships among Stokes parameters, rotary spectra and cross-spectral methods

Stephen D. Eckermann[1]

Computational Physics, Incorporated, Fairfax, Virginia

Abstract. The elliptical rotation with height of horizontal velocities produced by gravity waves provides considerable information about the wave field. Methods of statistically characterizing velocity ellipses from data currently fall into three main categories: (1) hodographic analyses, (2) cross-spectral analyses, and (3) rotary spectral analyses. The three methods have some intuitive similarities, yet precise interrelationships among them are presently unclear. The three techniques are interrelated here using the so-called "Stokes parameters" of the wave field, which initially provide a concise description of the hodographic analysis method (1). On Fourier transforming the Stokes parameters, standard formulae employed in rotary-spectral and cross-spectral analysis methods can then be expressed in terms of the resulting "Stokes-parameter spectra." The results highlight some drawbacks in the use of cross-coherence spectra between velocity components to verify the existence of a coherent wave motion. A more robust measure is suggested, based on the "degree of polarization" of classical hodograph-based Stokes-parameter analysis, which can be generalized to provide an analogous spectral measure for evaluation in rotary-spectral and cross-spectral analyses.

Introduction

It is well known that the horizontal-velocity motion ellipses produced by gravity waves can provide a lot of information on the wave field. For a single, linear, steady, nondissipating, plane wave in a region with negligible vertical shear in the background wind, the axial ratio of this motion ellipse can provide the intrinsic frequency of the wave, a parameter which is very difficult to measure any other way [e.g., *Cot and Barat*, 1986]. The horizontal propagation axis of the wave is given by the orientation of the ellipse major axis [*Vincent and Fritts*, 1987], while the sense of ellipse rotation with height provides the direction of the wave's vertical group velocity [e.g., *Hirota and Niki*, 1985; *Andrews et al.*, 1987]. In strongly sheared environments, ellipticity may also arise due to the interaction of the wave motion with the background velocity profile [*Hines*, 1989; *Cho*, 1995]. Consequently, a number of techniques have been developed which can quantify the elliptical properties of vertical profiles of horizontal velocity perturbations produced by gravity waves.

The first and most widely used method relies on forming hodographs from the velocity profiles. This is a straightforward and accurate technique when a large-amplitude monochromatic wave is present in a region of minimal background wind shear [e.g., *Cot and Barat*, 1986; *Muraoka et al.*, 1994]. However, actual velocity hodographs are usually irregular and variable, and so a number of hodographic algorithms have been developed which sort and classify a large number of profiles to yield a statistical picture of the wave field [e.g., *Hirota and Niki*, 1985; *Hamilton*, 1991; *Hall et al.*, 1995]. One particularly general form of the hodographic method is a description in terms of Stokes parameters [*Vincent and Fritts*, 1987], an approach we shall pursue here.

However, observations and models have suggested that a fairly broad spectrum of many waves is present on average [e.g., *Tsuda et al.*, 1991; *Hines*, 1991], whereas hodographic techniques require a single coherent wave to dominate the fluctuations within the profile. *Eckermann and Hocking* [1989] demonstrated that hodographic analyses of profiles which contained a large number of gravity waves sometimes gave results which reflected the statistical properties of random incoherent fluctuations, rather than the polarization characteristics of any waves in the data. Consequently, spectral techniques have been pursued which can search for coherent waves within various wavelength bands and, if any are identified, can isolate each wave and characterize it using hodographic methods.

First efforts along these lines concentrated on rotary spectra, which are power spectra of the complex velocity vector $u'(z) + iv'(z)$, where $u'(z)$ and $v'(z)$ are vertical profiles of the fluctuating zonal and meridional wind velocities, respectively. When plotted in the complex plane, the rotation of this "rotary vector" with height provides identical information to velocity hodographs. Thus generalized rotary-vector analysis methods have been developed [e.g., *Gonella*, 1972; *Hayashi*, 1979] and are used commonly in studies of oceanic gravity waves [e.g., *Artale and Gasparino*, 1990; *Plueddemann*, 1992]. When applied to gravity waves in the middle atmosphere, strong anisotropies between the clockwise-rotating and anticlockwise-rotating rotary spectral components were revealed at all vertical wavenumbers, which were consistent with a preponderance of upward propagating gravity wave packets [e.g., *Thompson*, 1978; *Cadet and Teitelbaum*, 1979; *Vincent*, 1984; *Hass and Meyer*, 1987; *Eckermann and Vincent*, 1989; *Thomas et al.*, 1992].

[1]Also at the E. O. Hulburt Center for Space Research, Naval Research Laboratory, Washington, DC.

Paper number 96JD01578.
0148-0227/96/96JD-01578$09.00

Report Documentation Page

Form Approved
OMB No. 0704-0188

1. REPORT DATE	2. REPORT TYPE	3. DATES COVERED
AUG 1996		**00-00-1996 to 00-00-1996**

4. TITLE AND SUBTITLE	5a. CONTRACT NUMBER
Hodographic analysis of gravity waves: Relationships among Stokes parameters, rotary spectra and cross-spectral methods	5b. GRANT NUMBER
	5c. PROGRAM ELEMENT NUMBER
6. AUTHOR(S)	5d. PROJECT NUMBER
	5e. TASK NUMBER
	5f. WORK UNIT NUMBER
7. PERFORMING ORGANIZATION NAME(S) AND ADDRESS(ES) **Naval Research Laboratory,E.O. Hulburt Center for Space Research,Washington,DC,20375**	8. PERFORMING ORGANIZATION REPORT NUMBER
9. SPONSORING/MONITORING AGENCY NAME(S) AND ADDRESS(ES)	10. SPONSOR/MONITOR'S ACRONYM(S)
	11. SPONSOR/MONITOR'S REPORT NUMBER(S)

12. DISTRIBUTION/AVAILABILITY STATEMENT
Approved for public release; distribution unlimited

13. SUPPLEMENTARY NOTES

14. ABSTRACT
see report

15. SUBJECT TERMS

16. SECURITY CLASSIFICATION OF:			17. LIMITATION OF ABSTRACT	18. NUMBER OF PAGES	19a. NAME OF RESPONSIBLE PERSON
a. REPORT **unclassified**	b. ABSTRACT **unclassified**	c. THIS PAGE **unclassified**	**Same as Report (SAR)**	**6**	

Eckermann and Vincent [1989] presented a spectral version of the Stokes-parameters method of characterizing gravity wave hodographs [*Vincent and Fritts*, 1987] and applied it to rocketsonde profiles of stratospheric velocities. The technique provided a "degree of polarization" measure for identifying coherent waves within any given wavenumber band as well as other hodograph-related measures of the polarization characteristics of coherent waves within various bands [*Eckermann and Vincent*, 1989; *Eckermann et al.*, 1995].

Recently, *Cho* [1995] has developed a cross-spectral technique, which, he argued, combined the advantages of the multiwave rotary-spectrum approach with the interpretive advantages of a hodographic analysis. On the latter property he noted that the technique was, in principle, a spectral analogue of the Stokes-parameters analysis. He employed the method to investigate the elliptical properties of the wave field measured by radar over Arecibo.

Clearly, all three spectral methods give similar results and must be related in some way. The purpose of this short paper is to explicate these relationships.

Hodographic Decomposition: Stokes Parameters

In hodographic analyses of gravity wave horizontal-velocity perturbations, velocities are plotted vectorally, and values at successive heights are interconnected. The resulting velocity hodographs frequently reveal elliptical wave-induced velocity "spirals" as a function of height [*Hirota and Niki*, 1985; *Cot and Barat*, 1986; *Yamanaka et al.*, 1996]. Various analysis techniques have been developed to identify and characterize large numbers of these hodographs in some statistical sense [*Hirota and Niki*, 1985; *Kitamura and Hirota*, 1989; *Hamilton*, 1991; *Hall et al.*, 1995].

One complete and concise formulation of this method is provided by the so-called Stokes parameters. This is a standard analysis technique for electromagnetic waves and is well described in standard texts from optics and radiophysics [e.g., *Kraus*, 1966; *Born and Wolf*, 1980]. An attractive feature of these parameters is that any partially polarized wave motion can be described completely and uniquely in terms of its Stokes parameters.

Vincent and Fritts [1987] were the first to advocate their usefulness in gravity wave studies. In this context the technique assumes that any given vertical profile of horizontal-velocity perturbations, $(u'(z), v'(z))$, contains a partially polarized wave field: that is, a single coherent wave is present, of peak amplitude (u_0, v_0), within an unpolarized, isotropic, noiselike background velocity field of variance $\overline{u^2_{\text{noise}}} + \overline{v^2_{\text{noise}}}$. The four Stokes parameters can then be defined as

$$I = \tfrac{1}{2}(\overline{u_0^2} + \overline{v_0^2}) + (\overline{u^2_{\text{noise}}} + \overline{v^2_{\text{noise}}}) = \overline{u'^2} + \overline{v'^2}, \quad (1)$$

$$D = \tfrac{1}{2}(\overline{u_0^2} - \overline{v_0^2}) = \overline{u'^2} - \overline{v'^2}, \quad (2)$$

$$P = \overline{u_0 v_0 \cos\delta} = 2\overline{u'v'}, \quad (3)$$

$$Q = \overline{u_0 v_0 \sin\delta}, \quad (4)$$

where overbars denote height and/or time averaging of the perturbation velocities; and δ is a phase defining the ellipticity of the wave: $\delta = 0°$ or 180° implies linear polarization ($Q = 0$), $\delta = 90°$ or 270° implies circular polarization ($P = 0$), and anything in between implies elliptical polarization. Thus P is the "in-phase" covariance associated with linear polarization, and Q is the "in quadrature" covariance associated with circular wave polarization, while I clearly quantifies the total variance and D defines its axial anisotropy.

Note that the isotropic noiselike variance in the profile does not contribute to D, P, or Q but does contribute to the total variance I. To discriminate between the wave and the noiselike contributions to I, a degree of polarization d can be defined which quantifies the fractional contribution of the coherent wave motion to the total velocity variance. Since $I^2 = D^2 + P^2 + Q^2$ for a single wave in the absence of noise, then it follows that

$$d = \frac{(D^2 + P^2 + Q^2)^{1/2}}{I}, \quad (5)$$

where $0 \le d \le 1$ and d is rotationally invariant, in that its value does not depend on the coordinate axes used to evaluate (1)–(4). A number of other useful parameters can also be calculated from the Stokes parameters [e.g., *Kraus*, 1966; *Born and Wolf*, 1980; *Eckermann and Vincent*, 1989].

Most Stokes-parameter definitions are a factor of 2 larger than those in (1)–(4) [*Vincent and Fritts*, 1987]. The inclusion of some constant scaling factor has no influence on the technique, and we adopt the present definitions because they make later correspondences with spectral quantities particularly simple.

Stokes-Parameter Spectra

The expressions (1)–(4), as given by *Vincent and Fritts* [1987], involve computing variances and covariances from the velocity profile. This has some disadvantages: for example, computing Q from definition (4) is not straightforward and was not attempted by *Vincent and Fritts* [1987] (*Eckermann et al.* [1995] noted that it can be achieved by Hilbert transforming one of the profiles). This profile-based form of the technique also assumes that one dominant wave exists in the data, whereas in atmospheric profiles, it is more usual to encounter a number of superposed waves [e.g., *Eckermann and Hocking*, 1989; *Riggin et al.*, 1995].

Analysis of profiles which contain more than one wave is clearly more suited to the Fourier domain, and *Vincent and Fritts* [1987] noted that Q as well as the other parameters might be calculable spectrally. This possibility was investigated and developed by *Eckermann and Vincent* [1989]. Given vertical profiles $u'(z)$ and $v'(z)$, as before, then Fourier transforming them over their full height ranges yields the following Fourier representations of the profiles:

$$\mathbf{U}(m) = U_R(m) + \imath U_I(m), \quad (6)$$

$$\mathbf{V}(m) = V_R(m) + \imath V_I(m), \quad (7)$$

where m is the vertical wavenumber, and the bold symbols denote a complex term. From here, *Eckermann and Vincent* [1989] derived the following power spectral densities for the four Stokes parameters, based on definitions (1)–(4):

$$\tilde{I}(m) = A(\overline{U_R^2(m)} + \overline{U_I^2(m)} + \overline{V_R^2(m)} + \overline{V_I^2(m)}), \quad (8)$$

$$\tilde{D}(m) = A(\overline{U_R^2(m)} + \overline{U_I^2(m)} - \overline{V_R^2(m)} - \overline{V_I^2(m)}), \quad (9)$$

$$\tilde{P}(m) = 2A(\overline{U_R(m)V_R(m)} + \overline{U_I(m)V_I(m)}), \quad (10)$$

$$\tilde{Q}(m) = 2A(\overline{U_R(m)V_I(m)} - \overline{U_I(m)V_R(m)}). \quad (11)$$

The overbars denote averages over some number of independent spectral realizations, to remove the effects of incoherent motions (for some types of data, this is either inappropriate or impossible), and A is a constant which scales the squared Fourier terms to power spectral densities. Consequently, any Stokes parameter X (one of I, D, P or Q) can now be evaluated over the full range of heights within any wavenumber band, according to Parseval's relation

$$X_{m_1,m_2} = \int_{m_1}^{m_2} \bar{X}(m)\, dm, \tag{12}$$

where X_{m_1,m_2} is one of the Stokes parameters (1)–(4) evaluated over a wavenumber band between m_1 and m_2 from its corresponding power spectral density $\bar{X}(m)$. This Fourier decomposition of the Stokes parameters clearly allows for more than one coherent wave to be isolated from any given sequence of velocity profiles, so long as the various coherent waves in the profile exist within well-defined and well-separated vertical-wavenumber bands.

Note that (8) is just the total horizontal-velocity autospectrum, (9) is the difference between the component autospectra, and (10) and (11) are twice the real and imaginary components of the total velocity cospectrum (as discussed below). These spectral expressions are closely related to the various components of the classical "coherency matrix," which can also be used to quantify the Stokes parameters [*Born and Wolf*, 1980]: indeed, a direct analogy was provided by *Calman* [1978a] through a "spectrum density matrix," which he used to characterize various types of polarized oceanic wave motions. The key point here is that when coherent waves are present and well separated from each other in Fourier space, standard autospectra and cospectra of the profiles provide fundamental information about the polarization characteristics of these waves. The usefulness of this analogy is demonstrated in the next two sections, where some other spectral formulae which are commonly used to analyze gravity wave fields are expressed in terms of the "Stokes-parameter spectra" (8)–(11).

Stokes-Parameter Spectra and the Cross-Spectral Method

Of particular interest here are the expressions for $\tilde{P}(m)$ and $\tilde{Q}(m)$, which are, respectively, twice the "in-phase" and "in-quadrature" correlation spectra between the vertical profiles $u'(z)$ and $v'(z)$. Because of their orthogonality implied by (3) and (4), they can be combined into a complex vector

$$\tilde{\mathbf{C}}(m) = \tilde{P}(m) + \iota\tilde{Q}(m) = \tilde{T}(m)\, \exp\,[\iota\tilde{\Phi}(m)], \tag{13}$$

where $\tilde{\mathbf{C}}(m)$ is twice the total cross spectrum between $u'(z)$ and $v'(z)$, $\tilde{T}^2(m) = \tilde{P}^2(m) + \tilde{Q}^2(m)$, and

$$\tilde{\Phi}(m) = \arctan\left(\frac{\tilde{Q}(m)}{\tilde{P}(m)}\right). \tag{14}$$

We then normalize (13) to form the cross-coherence spectrum [e.g., *Fofonoff*, 1969]

$$\tilde{\mathbf{S}}(m) = \frac{\tilde{\mathbf{C}}(m)}{2A|\mathbf{U}(m)|\,|\mathbf{V}(m)|}. \tag{15}$$

$\tilde{\mathbf{S}}(m)$ is used in the cross-spectral analysis method of *Cho* [1995]. With the aid of (8)–(11) and (13), (15) can be reexpressed entirely in terms of the Stokes-parameter spectra, yielding

$$\tilde{\mathbf{S}}(m) = \left(\frac{\tilde{P}^2(m) + \tilde{Q}^2(m)}{\tilde{I}^2(m) - \tilde{D}^2(m)}\right)^{1/2} \exp\,[\iota\tilde{\Phi}(m)]. \tag{16}$$

Thus the correspondence between Cho's cross-spectral method and the hodograph-based Stokes-parameters method is given by (14) and (16). Several points are now worth noting.

First, the cross-spectral method of *Cho* [1995] makes most use of the cross-spectral phase $\tilde{\Phi}(m)$. Note that it is the spectral analogue of the δ term in (3) and (4), as *Eckermann and Vincent* [1989] demonstrated (see their equation (7)). On assuming $-180° \leq \tilde{\Phi}(m) \leq 180°$, then *Cho* [1995] argued that the sign of $\tilde{\Phi}(m)$ yielded the sense of elliptical velocity-vector rotation with height, whereas in Stokes-parameter analyses, the sign of $\tilde{Q}(m)$ is used [*Eckermann and Vincent*, 1989; *Eckermann et al.*, 1995]. The two approaches are seen to be equivalent on inspecting (14), since the sign of $\tilde{\Phi}(m)$ is determined solely by the sign of $\tilde{Q}(m)$.

Cho [1995] also advocated using the magnitude of $\tilde{\mathbf{S}}(m)$ (where $\tilde{\mathbf{S}}(m)$ has been suitably averaged over a number of independent spectral realizations) to verify the presence of a coherent wave event within any spectral band. This requires both height and time resolution, so that spectra calculated from height (time) profiles can be averaged with respect to time (height). It is more usual to investigate the cross coherence between two time series of a given quantity which are recorded at displaced locations, to infer a "coherence length" of the recorded phenomenon [e.g., *Madden and Julian*, 1972; *Briscoe*, 1975; *Pinkel*, 1975; *Reid and Vincent*, 1987].

$|\tilde{\mathbf{S}}(m)|$, on the other hand, quantifies the coherence between the two orthogonal components of a single-vector time series. This leads to problems which are analogous to those encountered when one uses the correlation coefficient between $u'(z)$ and $v'(z)$ (a normalized version of P in (3)) to infer azimuthal wave field anisotropy, as discussed in section 3.2 of *Eckermann and Vincent* [1989]. As an illustration of the problem, consider a profile containing a single linearly polarized wave aligned either zonally or meridionally, which implies $P = Q = 0$. According to (13) this wave has a vanishing cross spectrum and therefore an undefined cross coherence (15) (adding some noise eliminates this singularity, giving a vanishing cross coherence). Yet clearly, a 100%-coherent wave motion is present. This weakness in the cross-coherence technique can be avoided by rotating the coordinate axes through successive angles and recalculating the cross-coherence spectra each time [*Eckermann and Vincent*, 1989].

To illustrate the problem, Figure 1 compares the cross-spectral and Stokes-parameter methods of inferring coherence, based on synthesized profiles containing a coherent wave plus noise. In Stokes-parameter analysis a coherent wave is identified through the degree of polarization (5), so that, within a wavenumber band $m_1 \leq m \leq m_2$,

$$d_{m_1,m_2} = \frac{(D^2_{m_1,m_2} + P^2_{m_1,m_2} + Q^2_{m_1,m_2})^{1/2}}{I_{m_1,m_2}}. \tag{17}$$

Note from Figure 1 that both techniques give the same results when the semimajor axis of the wave ellipse is aligned to 45° to the coordinate axes. However, when the same wave is oriented either north-south or east-west, the cross-coherence method loses sensitivity, whereas d_{m_1,m_2} remains insensitive to

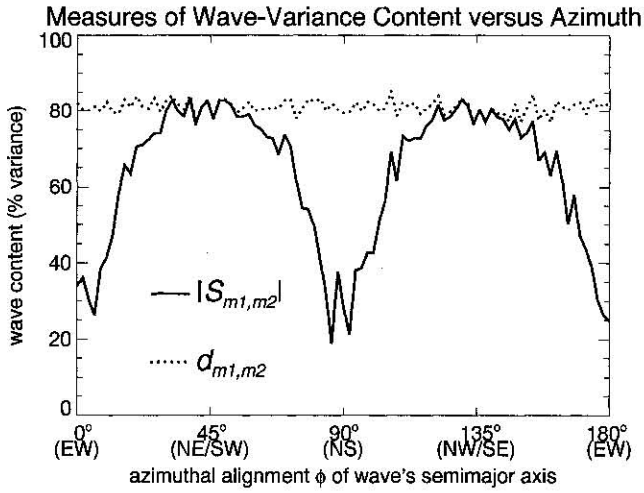

Figure 1. Comparison of the cross coherence $|S_{m_1,m_2}|(=|\int_{m_1}^{m_2} \tilde{\mathbf{S}}(m)\, dm|)$ and degree of polarization d_{m_1,m_2}, as computed from synthesized data. The synthesized vertical profiles contained an elliptically polarized wave ($|f/\omega| = 0.1$, where ω is intrinsic frequency and f is inertial frequency) with a total horizontal-velocity variance of 25.25 $m^2\ s^{-2}$ and a vertical wavelength of 4 km. The semimajor axis of this coherent wave was aligned at an azimuth angle ϕ and then sampled over a total height range of 40 km, and at a vertical resolution is 1 km to give two profiles of zonal and meridional velocities. Uncorrelated Gaussian noise with a variance of 10 $m^2\ s^{-2}$ was added to both the zonal and the meridional profiles. One hundred independent pairs of zonal and meridional velocity profiles were analyzed spectrally within a wavenumber band between $m_1 = 2\pi\ (5\ \text{km})^{-1}$ and $m_2 = 2\pi\ (3\ \text{km})^{-1}$.

the wave's azimuthal alignment. These properties of $|\tilde{\mathbf{S}}(m)|$ and d_{m_1,m_2} can be used to relate the two, as noted in Appendices B and C of *Hayashi* [1979]. The relation in terms of Stokes-parameter spectra is

$$|\tilde{\mathbf{S}}(m)|^2 = \frac{\tilde{I}^2(m)\tilde{d}^2(m) - \tilde{D}^2(m)}{\tilde{I}^2(m) - \tilde{D}^2(m)}, \tag{18}$$

where

$$\tilde{d}^2(m) = \frac{\tilde{D}^2(m) + \tilde{P}^2(m) + \tilde{Q}^2(m)}{\tilde{I}^2(m)}. \tag{19}$$

Note that (18) reproduces the earlier result: that a linearly polarized wave aligned either north-south and east-west ($\tilde{P}(m) = \tilde{Q}(m) = 0$) has an undefined cross coherence in the absence of noise ($\tilde{d}(m) = 1$) and a vanishing cross coherence when some noise variance is present ($0 < \tilde{d}(m) < 1$).

The sensitivity of $|\tilde{\mathbf{S}}(m)|$ to ellipse orientation was highlighted in oceanographic studies by *Fofonoff* [1969], who presented some alternative measures which were invariant under coordinate rotations. This stimulated efforts to identify other quantities which were similarly insensitive to coordinate specifics and led to the development of the rotary-vector method [*Gonella*, 1972], which we investigate next.

Stokes Parameters and the Rotary Spectrum

The Stokes parameters are, of course, not the only way in which gravity wave velocity hodographs can be objectively characterized [e.g., *Hamilton*, 1991]. Another quite general approach is the rotary-vector method, which has proved a popular tool in oceanic studies of gravity waves [e.g., *Artale and Gasparino*, 1990; *D'Asaro and Morehead*, 1991; *Plueddemann*, 1992]. The rotary-vector method utilizes the complex velocity phasor $u'(z) + \iota v'(z)$ and provides a number of different parameters which describe various aspects of the wave polarization [e.g., *Gonella*, 1972; *Calman*, 1978b]. However, in atmospheric studies to date, only the rotary spectrum has been calculated with any sort of regularity [e.g., *Thompson*, 1978; *Cadet and Teitelbaum*, 1979; *Vincent*, 1984; *Hass and Meyer*, 1987; *Thomas et al.*, 1992], and so we shall focus mostly on this quantity. Treatises on the rotary-vector method and its correspondences with various hodographic and cross-spectral terms are given by *Gonella* [1972], *Mooers* [1973], *Calman*, [1978a], and *Hayashi* [1979].

Rotary spectra are derived by first Fourier transforming $u'(z) + \iota v'(z)$, yielding a Fourier transform $\mathbf{R}(m)$. Clockwise-rotating and anticlockwise-rotating circular phasors then partition to the negative and positive wavenumbers, respectively, of $\mathbf{R}(m)$, so that one can evaluate clockwise-rotating ($C\tilde{W}(m)$) and anticlockwise-rotating ($A\check{C}W(m)$) power spectral densities according to

$$C\tilde{W}(m) = \frac{A}{2}\mathbf{R}^*(-m)\mathbf{R}(-m), \tag{20}$$

$$A\check{C}W(m) = \frac{A}{2}\mathbf{R}^*(m)\mathbf{R}(m), \tag{21}$$

where asterisks denote complex conjugation [*Leaman and Sanford*, 1975; *Vincent*, 1984]. The factor of two in (20) and (21) is needed since both positive and negative harmonics of the Fourier transform are used here, whereas only one side of the Fourier transform is used in (8)–(11) because (6)–(7) are Hermitian. The total autospectrum (equal to $\tilde{I}(m)$) is given by $C\tilde{W}(m) + A\check{C}W(m)$ [*Leaman and Sanford*, 1975].

Standard formulae interrelate the amplitudes of the zonal and meridional time series to clockwise-rotating and anticlockwise-rotating circular velocity phasors, and Fourier transforming them yields relations among the rotary spectral components and the autospectra and cospectra of $u'(z)$ and $v'(z)$ [*Gonella*, 1972; *Mooers*, 1973; *Calman*, 1978a]. Given the definitions (8)–(11) of the Stokes-parameter spectra and their earlier stated connections with autospectra and cospectra, then these results can be used to relate the rotary spectra to the Stokes-parameter spectra. The results are

$$C\tilde{W}(m) = \tfrac{1}{2}[\tilde{I}(m) - \tilde{Q}(m)], \tag{22}$$

$$A\check{C}W(m) = \tfrac{1}{2}[\tilde{I}(m) + \tilde{Q}(m)]. \tag{23}$$

Note that $\tilde{I}(m) = C\tilde{W}(m) + A\check{C}W(m)$, as required.

The above expressions have some practical advantages. For example, a conventional rotary spectrum estimate involves filtering the raw data using fast Fourier transform (FFT) methods (two FFTs, followed by two inverse FFTs) and then retransforming $u'(z) + \iota v'(z)$ [e.g., *Vincent*, 1984], a total of five FFTs. A rotary spectrum calculated directly from the Stokes-parameter spectra (8) and (11) of the raw data, using (22) and (23), requires only two FFTs.

As in the cross-spectral method, it is also common in the rotary-vector method to evaluate a cross-coherence spectrum $\tilde{\mathbf{S}}_{\pm}(m)$ between clockwise-rotating and anticlockwise-rotating velocity components [e.g., *Fofonoff*, 1969; *Gonella*, 1972; *Ha-*

yashi, 1979]. This coherence measure can also be expressed solely in terms of Stokes-parameter spectra, as follows:

$$\tilde{\mathbf{S}}_{\pm}(m) = \left(\frac{\tilde{D}^2(m) + \tilde{P}^2(m)}{\bar{I}^2(m) - \bar{Q}^2(m)} \right)^{1/2} \exp\left[\iota \tilde{\Phi}_{\pm}(m)\right], \quad (24)$$

where

$$\tilde{\Phi}_{\pm}(m) = \arctan\left(\frac{\tilde{P}(m)}{\tilde{D}(m)} \right). \quad (25)$$

Analogous derivations in terms of autospectra and cospectra are given by *Gonella* [1972] and *Mooers* [1973]. Similar relations are also given by *Calman* [1978a] and *Hayashi* [1979], but they use a different sign convention in defining their rotary-component cross-coherence spectrum, producing a phase of opposite sign to (25).

For a single wave of vertical wavenumber m_1 in a given sequence of profiles, then $\tilde{\Phi}_{\pm}(m_1) = 2\tau$, where τ is the azimuthal alignment of the wave's semimajor ellipse axis as given by the Stokes parameters [e.g., *Kraus*, 1966; *Vincent and Fritts*, 1987; *Eckermann and Vincent*, 1989]. This was noted by *Gonella* [1972], who then referred to $|\tilde{\mathbf{S}}_{\pm}(m)|$ as the stability (coherence) of the ellipse orientation (see also *Mooers* [1973]). Thus the rotary method can be used to investigate horizontal as well as vertical wave propagation directions and many other aspects of the wave field.

However, note once again that the rotary-component cross coherence is not a sensitive measure of the presence or absence of a coherent wave: for example, a circularly polarized wave ($P = D = 0$) in the presence of some noise variance always yields $|\tilde{\mathbf{S}}_{\pm}(m)| = 0$, since either the clockwise or the anticlockwise rotary component vanishes in this case. To identify coherent waves using the rotary-vector method, the spectral degree of polarization (19) can be calculated from the rotary-component spectra according to [*Hayashi*, 1979]

$$1 - \tilde{d}^2(m) = \frac{4\mathrm{A\check{C}W}(m)C\tilde{W}(m)}{[\mathrm{A\check{C}W}(m) + C\tilde{W}(m)]^2}[1 - |\tilde{\mathbf{S}}_{\pm}(m)|^2]. \quad (26)$$

Summary and Conclusions

Continuing improvements in the accuracy and resolution of data from atmospheric profiling instruments holds the promise of a wealth of new data on atmospheric gravity waves [e.g., *Hoppe and Fritts*, 1995; *Gardner et al.*, 1995; *Hamilton and Vincent*, 1995]. Parallel theoretical developments now mean that spectral analysis of these data will be a key tool in the appraisal of various theories of the wave field [e.g., *Fritts and Hoppe*, 1995; *Gardner et al.*, 1995]. Some theoretical models suggest that these wave spectra result from coherent large-amplitude waves with modulated intrinsic parameters [e.g., *Sato and Yamada*, 1994; *Alexander*, 1996; *Warner and McIntyre*, 1996], while others conclude that they are produced by an incoherent spectrum of many randomly interacting waves [e.g., *Hines*, 1991; *Medvedev and Klaassen*, 1995]. In assessing these and other issues through data analysis, the coherence, polarization, and energetics of the wave field are pertinent and can be quantified using a number of standard analysis techniques. It is important that the relationships among these techniques are clear so that firm conclusions can be drawn.

By using expressions for the power spectral densities of the four Stokes parameters [*Eckermann and Vincent*, 1989], relationships among the autospectra, cross spectra, and rotary spectra of wave-induced horizontal-velocity perturbations have been presented. Since the Stokes parameters provide information about the polarization characteristics of any coherent gravity waves in the data, these relationships aid interpretation of the data provided by cross-spectral and rotary-spectral analyses. The techniques are complementary but have different strengths and weaknesses. In particular, it was demonstrated here that cross-coherence measures between components of a single-vector series are, in general, unreliable indicators of the presence of a coherent wave in a given data set: a spectral "degree of polarization" measure was presented for future studies using any of the above methods.

There are many more, potentially useful, spectral quantities which can provide further information on the wave field [e.g., *Mooers*, 1973; *Calman*, 1978a, b; *Hayashi*, 1979]. The information provided by these more derived measures should also be interpretible through the relationships among the basic hodographic, cross-spectral, and rotary-spectral quantities discussed both here and elsewhere.

Acknowledgments. Many thanks to Mary Anderson at Computational Physics, Incorporated, for her administrative assistance.

References

Alexander, M. J., A simulated spectrum of convectively generated gravity waves: Propagation from the tropopause to the mesopause and effects on the middle atmosphere, *J. Geophys. Res.*, *101*, 1571–1588, 1996.

Andrews, D. G., J. R. Holton, and C. B. Leovy, *Middle Atmosphere Dynamics*, 489 pp., Academic, San Diego, Calif., 1987.

Artale, V., and G. P. Gasparino, Simultaneous temperature and velocity measurements of the internal wave field in the Corsican channel (eastern Ligurian Sea), *J. Geophys. Res.*, *95*, 1635–1645, 1990.

Born, M., and E. Wolf, *Principles of Optics*, 6th ed., 808 pp., Pergamon, New York, 1980.

Briscoe, M. G., Preliminary results from the trimoored internal wave experiment (IWEX), *J. Geophys. Res.*, *80*, 3872–3884, 1975.

Cadet, D., and H. Teitelbaum, Observational evidence of internal inertia-gravity waves in the tropical stratosphere, *J. Atmos. Sci.*, *36*, 892–907, 1979.

Calman, J., On the interpretation of ocean current spectra, I, The kinematics of three-dimensional vector time series, *J. Phys. Oceanogr.*, *8*, 627–643, 1978a.

Calman, J., On the interpretation of ocean current spectra, II, Testing dynamical hypotheses, *J. Phys. Oceanogr.*, *8*, 644–652, 1978b.

Cho, J. Y. N., Inertio-gravity wave parameter estimation from cross-spectral analysis, *J. Geophys. Res.*, *100*, 18,727–18,737, 1995.

Cot, C., and J. Barat, Wave-turbulence interaction in the stratosphere: A case study, *J. Geophys. Res.*, *91*, 2749–2756, 1986.

D'Asaro, E. A., and M. D. Morehead, Internal waves and velocity fine structure in the Arctic Ocean, *J. Geophys. Res.*, *96*, 12,725–12,738, 1991.

Eckermann, S. D., and W. K. Hocking, Effect of superposition on measurements of atmospheric gravity waves: A cautionary note and some reinterpretations, *J. Geophys. Res.*, *94*, 6333–6339, 1989.

Eckermann, S. D., and R. A. Vincent, Falling sphere observations of anisotropic gravity wave motions in the upper stratosphere over Australia, *Pure Appl. Geophys.*, *130*, 509–532, 1989.

Eckermann, S. D., I. Hirota, and W. K. Hocking, Gravity wave and equatorial wave morphology of the stratosphere derived from long-term rocket soundings, *Q. J. R. Meteorol. Soc.*, *121*, 149–186, 1995.

Fofonoff, N. P., Spectral characteristics of internal waves in the ocean, *Deep Sea Res.*, *16*(suppl.), 58–71, 1969.

Fritts, D. C., and U.-P. Hoppe, High-resolution measurements of vertical velocity with the European incoherent scatter VHF radar, 2, Spectral observations and model comparisons, *J. Geophys. Res.*, *100*, 16,827–16,838, 1995.

Gardner, C. S., X. Tao, and G. C. Papen, Simultaneous lidar observations of vertical wind, temperature, and density profiles in the upper

mesosphere: Evidence for nonseparability of atmospheric perturbation spectra, *Geophys. Res. Lett.*, *22*, 2877–2880, 1995.

Gonella, J., A rotary-component method for analysing meteorological and oceanographic vector time series, *Deep Sea Res.*, *19*, 833–846, 1972.

Hall, G. E., C. E. Meek, and A. H. Manson, Hodograph analysis of mesopause region winds observed by three MF radars in the Canadian prairies, *J. Geophys. Res.*, *100*, 7411–7421, 1995.

Hamilton, K., Climatological statistics of stratospheric inertia-gravity waves deduced from historical rocketsonde wind and temperature data, *J. Geophys. Res.*, *96*, 20,831–20,839, 1991.

Hamilton, K., and R. A. Vincent, High-resolution radiosonde data offer new prospects for research, *Eos Trans. AGU*, *76*(16), Spring Meet. Suppl., 506–507, 1995.

Hass, H., and W. Meyer, Gravity wave fields above Andøya, *J. Atmos. Terr. Phys.*, *49*, 705–721, 1987.

Hayashi, Y., Space-time spectral analysis of rotary-vector series, *J. Atmos. Sci.*, *36*, 757–766, 1979.

Hines, C. O., Tropopausal mountain waves over Arecibo: A case study, *J. Atmos. Sci.*, *46*, 476–488, 1989.

Hines, C. O., The saturation of gravity waves in the middle atmosphere, II, Development of Doppler-spread theory, *J. Atmos. Sci.*, *48*, 1360–1379, 1991.

Hirota, I., and T. Niki, A statistical study of inertia-gravity waves in the middle atmosphere, *J. Meteorol. Soc. Jpn.*, *63*, 1055–1066, 1985.

Hoppe, U.-P., and D. C. Fritts, High-resolution measurements of vertical velocity with the European incoherent scatter VHF radar, 1, Motion field characteristics and measurement biases, *J. Geophys. Res.*, *100*, 16,813–16,825, 1995.

Kitamura, Y., and I. Hirota, Small-scale disturbances in the lower stratosphere revealed by daily rawin sonde analysis, *J. Meteorol. Soc. Jpn.*, *67*, 817–830, 1989.

Kraus, J. D., *Radioastronomy*, 481 pp., McGraw-Hill, New York, 1966.

Leaman, K. D., and T. B. Sanford, Vertical energy propagation of inertial waves: A vector spectral analysis of velocity profiles, *J. Geophys. Res.*, *80*, 1975–1978, 1975.

Madden, R. A., and P. R. Julian, Description of global-scale circulation cells in the tropics with a 40–50 day period, *J. Atmos. Sci.*, *29*, 1109–1123, 1972.

Medvedev, A. S., and G. P. Klaassen, Vertical evolution of gravity wave spectra and the parameterization of associated wave drag, *J. Geophys. Res.*, *100*, 25,841–25,853, 1995.

Mooers, C. N. K., A technique for the cross spectrum analysis of pairs of complex-valued time series, with emphasis on the properties of polarized components and rotational invariants, *Deep Sea Res.*, *20*, 1129–1141, 1973.

Muraoka, Y., S. Fukao, T. Sugiyama, M. Yamamoto, T. Nakamura, T. Tsuda, and S. Kato, Features of a mesospheric inertio-gravity wave observed with the MU radar, *J. Atmos. Terr. Phys.*, *56*, 1163–1171, 1994.

Pinkel, R., Upper ocean internal wave observations from Flip, *J. Geophys. Res.*, *80*, 3892–3910, 1975.

Plueddemann, A. J., Internal wave observations from the Arctic environmental drifting buoy, *J. Geophys. Res.*, *97*, 12,619–12,638, 1992.

Reid, I. M., and R. A. Vincent, Measurements of the horizontal scales and phase velocities of short period mesospheric gravity waves at Adelaide, Australia, *J. Atmos. Terr. Phys.*, *49*, 1033–1048, 1987.

Riggin, D., D. C. Fritts, C. D. Fawcett, and E. Kudeki, Observations of inertia-gravity wave motions in the stratosphere over Jicamarca, Peru, *Geophys. Res. Lett.*, *22*, 3239–3242, 1995.

Sato, K., and M. Yamada, Vertical structure of atmospheric gravity waves revealed by the wavelet analysis, *J. Geophys. Res.*, *99*, 20,623–20,631, 1994.

Thomas, L., I. T. Pritchard, and I. Astin, Radar observations of an inertia-gravity wave in the troposphere and lower stratosphere, *Ann. Geophys.*, *10*, 690–697, 1992.

Thompson, R. O. R. Y., Observation of inertial waves in the stratosphere, *Q. J. R. Meteorol. Soc.*, *104*, 691–698, 1978.

Tsuda, T., T. E. VanZandt, M. Mizumoto, S. Kato, and S. Fukao, Spectral analysis of temperature and Brunt-Väisälä frequency fluctuations observed by radiosondes, *J. Geophys. Res.*, *96*, 17,265–17,278, 1991.

Vincent, R. A., Gravity-wave motions in the mesosphere, *J. Atmos. Terr. Phys.*, *46*, 119–128, 1984.

Vincent, R. A., and D. C. Fritts, A climatology of gravity wave motions in the mesopause region at Adelaide, Australia, *J. Atmos. Sci.*, *44*, 748–760, 1987.

Warner, C. D., and M. E. McIntyre, On the propagation and dissipation of gravity-wave spectra through a realistic middle atmosphere, *J. Atmos. Sci.*, in press, 1996.

Yamanaka, M. D., S. Ogino, S. Kondo, T. Shimomai, S. Fukao, Y. Shibagaki, Y. Maekawa, and I. Takayabu, Inertio-gravity waves and subtropical multiple tropopauses: Vertical wavenumber spectra of wind and temperature observed by the MU radar, radiosondes and operational rawinsonde network, *J. Atmos. Terr. Phys.*, *58*, 785–805, 1996.

S. D. Eckermann, c/o E. O. Hulburt Center for Space Research, Code 7641, Naval Research Laboratory, Washington, D. C. 20375. (e-mail: eckerman@ismap4.nrl.navy.mil; WWW: http://rdpsvr.nrl.navy.mil.)

(Received January 30, 1996; revised May 7, 1996;
accepted May 7, 1996.)